Photochemistry and Photobiology, 2008, 84: 620–626

Solvochromic Effects in Model Eumelanin Compounds†

Stephen P. Nighswander-Rempel*[1], Indumathy B. Mahadevan[1], Paul V. Bernhardt[2], Jessica Butcher[1] and Paul Meredith[1]

[1]Centre for Organic Photonics and Electronics, School of Physical Sciences, University of Queensland, Brisbane, Queensland, Australia
[2]School of Molecular and Microbial Sciences, University of Queensland, Brisbane, Queensland, Australia

Received 30 October 2007, accepted 8 December 2007, DOI: 10.1111/j.1751-1097.2007.00290.x

ABSTRACT

We have created an indolic compound which is ideally suited to the study of the relationship between structure and function in eumelanin formation. *N*-methyl-5-hydroxy-6-methoxyindole (MHMI) is stable in solid and liquid states, highly soluble in a variety of solvents and forms a dimer only through the 4-4′ positions. The limited binding possibilities are due to functional groups strategically placed to inhibit chemical interactions through the 2 and 7 positions. It forms a crystal structure with a remarkable packing arrangement, with four monomers grouped in parallel pairs spaced 3.5 Å apart within each unit cell. Optical spectra reveal a multi-peaked absorbance profile similar to 5,6-dihydroxyindole (DHI) and *N*-acetyl-tryptophanamide (NATA), and strong fluorescence emission with radiative quantum yields of 29% and 33% in benzene and acetonitrile, respectively. The quantum yield is similar to that of 5,6-dihydroxyindole-2-carboxylic acid (DHICA) and shows that solvent aromaticity by itself does not affect the yield. Solution in chloroform results in an almost complete quenching of the fluorescence but an increase in emission is observed with photoactivation. Crystallographic results shown here suggest new structural possibilities for eumelanin and the controlled binding possibilities make this an excellent model for monitoring changes in function with increasing oligomer size in eumelanin formation.

INTRODUCTION

Eumelanin is a primary pigment which plays important photoprotective roles in human skin. It is able to protect us from the damaging effects of solar UV radiation because of its broad absorbance profiles, its extremely low quantum yield and its antioxidant and free radical-scavenging behavior (1–3). The cause of these highly unusual spectroscopic properties has been the source of much debate, but recent work has shown them to result from chemical disorder in the primary and secondary structures (4–6). This is supported by recent work on humic substances, whose absorbance, emission and radiative quantum yield properties are remarkably similar to those of eumelanin and similarly attributed to structural disorder (7).

Eumelanin is known to consist of macromolecules of 5,6-dihydroxyindole (DHI), 5,6-dihydroxyindole-2-carboxylic acid (DHICA) and their oxidized forms. How these units are arranged within the larger eumelanin complex remains uncertain, and indeed, there are a variety of ways in which complexes have been suggested to form (8–10). It seems likely that a variety of macromolecules do form and that this diversity, or disorder, lies at the heart of eumelanin's functionality. Indeed, these macromolecules could be responsible for the low radiative quantum yield, as recent studies have shown that quantum yield decreases not only with aggregation (11,12) but also with increasing particle size (13).

In order to understand the relationship between macromolecular size and spectroscopic properties more fully, it would be useful to monitor the spectroscopic properties of one of these molecules at several levels of polymerization. However, this is challenging with DHI and DHICA because DHI tends to react even under mild conditions, making it difficult to obtain pure monomeric or dimeric samples (12), and DHICA dimerizes in the 4, 7 and possibly even the 3 position, yielding several structurally and possibly optically distinct compounds (14,15). In this report, we present a new compound, *N*-methyl-5-hydroxy-6-methoxyindole (MHMI), which is ideally suited for such studies, and we examine its properties using crystallography, spectroscopy and nuclear magnetic resonance. This compound has a methyl group attached to the nitrogen in the pyrrole ring, and a hydroxy group and a methoxy group attached to the 5 and 6 positions, respectively, in the benzene ring (Fig. 1). It is an ideal model for studying eumelanin formation and functionality because the presence of these functional groups sterically restricts the number of binding sites, allowing greater control over the possible dimeric and polymeric species created and greater uniformity than can be found in natural eumelanin.

MHMI exhibits spectroscopic properties similar to DHICA, interesting stacking features which shed light on possible eumelanin structural arrangements, and significant solvochromic behavior. The latter was examined using aromatic (benzene) and nonaromatic solvents (acetonitrile and chloroform), showing that solvent aromaticity by itself has little effect on radiative quantum yield. Yields for the compound in chloroform were orders of magnitude lower than in the other

†This invited paper is part of the Symposium-in-Print: Melanins.

*Corresponding author email: snighrem@physics.uq.edu.au (Stephen P. Nighswander-Rempel)

© 2008 The Authors. Journal Compilation. The American Society of Photobiology 0031-8655/08

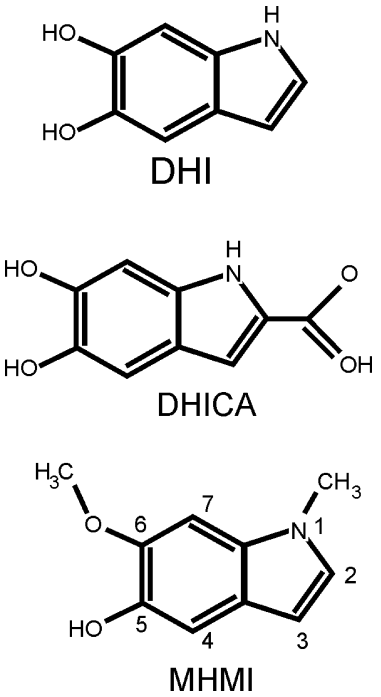

Figure 1. Structures of indolic compounds. Numeric labeling of the indole positions is included for discussion in the text.

solvents and we examine the chemical interactions responsible for that. Results for dimeric and oligomeric forms of MHMI will be published separately.

MATERIALS AND METHODS

Compound synthesis. 5-Benzyloxy-6-methoxyindole purchased from Sigma Aldrich was *N*-methylated in dry DMF using sodium hydride as the base and methyl iodide as the alkylating agent. The reaction was carried out under an atmosphere of argon for 2 h. The *N*-methyl-5-benzyloxy-6-methoxyindole (MBMI) thus obtained was subjected to hydrogenolysis for 3 h in ethyl acetate–acetic acid solution, using 5% palladium on carbon as catalyst to furnish MHMI monomer. The crude product thus obtained was purified over a column of silica using chloroform as eluant, and then crystallized from dichloromethane-hexane. A series of solutions ranging in concentration from 0.5 to 10 μM were prepared in each of benzene, acetonitrile and chloroform.

Crystallography. Intensity data at 293 K were collected on an Enraf-Nonius CAD4 four-circle diffractometer using graphite monochromated Mo-Kα radiation (λ = 0.71073 Å) in the ω-2θ scan mode. Lattice dimensions were determined by a least squares fit of the setting parameters of 25 independent reflections. Data reduction was performed with the WINGX package (16). The structure was solved by direct methods with SHELXS and refined by full matrix least squares analysis with SHELXL97 (17). All non-H atoms were refined with anisotropic thermal parameters, and H-atoms were constrained at estimated positions. The atomic nomenclature is defined in Fig. 2, drawn with ORTEP-3 (18) while the packing diagrams (Fig. 3) were drawn with PLATON (19). CCDC 657032 contains the supplementary crystallographic data for this paper in CIF format. These data can be obtained free of charge at http://www.ccdc.cam.ac.uk/conts/retrieving.html.

MHMI: $C_{10}H_{11}O_2$, M 177.20, T 293 K, monoclinic, space group $P2_1/a$ (No. 14, variant of $P2_1/c$), a 13.928(2) Å, b 10.520(2) Å, c 24.782(2) Å, β 93.47(1)°, V 3625(1) Å^3, D_c (Z = 16) 1.299 g cm^{-3}, F(000) 1504, μ(Mo Kα) 0.91 cm^{-1}, 6262 unique data ($2\theta_{max}$ = 50°), R_{int} = 0.0476, 1511 with $I > 2\sigma(I)$; R 0.0830 (obs. data), wR_2 0.2863 (all data), goodness-of-fit 0.935.

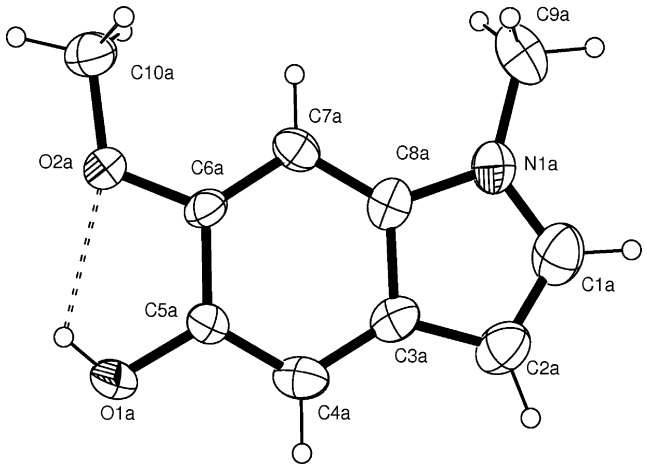

Figure 2. ORTEP3 diagram of a single molecule (A) from the structure (30% probability ellipsoids are shown). Note that numeric position labeling used by ORTEP is different from that found in Fig. 1 and used roufinely in melanin literature, particularly with respect to positions 2 and 3.

Optical spectroscopy. Absorbance spectra were recorded using a Cary (Palo Alto, CA) 300 spectrophotometer with a 600 nm min^{-1} scan speed and 2 nm spectral bandwidth. All spectra were collected using a 1 cm square quartz cuvette. Solvent scans (obtained under identical conditions) were used for background correction. Fluorescence emission spectra were recorded using a Jobin Yvon (Edison, NJ) Fluoromax 3 fluorimeter with a 2 nm bandpass, an integration time of 0.5 s and an excitation wavelength of 300 nm. Solvent scans were again performed under identical instrumental conditions for background correction. All emission spectra were corrected for reabsorption and inner filter effects using the method outlined previously (3). Quantum yields were calculated using the method described previously (20) and quinine sulfate as a reference standard (21). As the quantum yield of quinine is temperature-dependent, the ambient temperature surrounding the cuvette was measured to be 35°C, resulting in a 2.5% shift from the published value of 0.546.

NMR spectroscopy. ^{1}H NMR and ^{13}C NMR spectra were recorded on a Bruker Digital Avance-500 NMR spectrometer, in d_4-methanol. The chemical shifts are reported in p.p.m. relative to d_4-methanol, 3.30 p.p.m. for proton and 49.0 p.p.m. for ^{13}C.

RESULTS

The crystal structure of MHMI was determined by X-ray diffraction. Curiously, the compound crystallizes with four distinct MHMI monomers in the asymmetric unit. Each molecule (A, B, C and D) exhibits the same conformation and interatomic dimensions within experimental uncertainty and a view of one of these (molecule A) is shown in Fig. 2. There is an acute intramolecular H-bond between the hydroxyl and methoxyl groups. The packing is remarkable (Fig. 3a) and shows that the four distinct molecules are organized into parallel pairs offset from one another (Fig. 3b). The interplanar separations between the pairs span the range 3.46–3.55 Å. This is nearly identical to the 3.45 Å spacing previously inferred from X-ray scattering studies and applied to a stacking model in amorphous eumelanin (22). It can be seen that each monomer is related by a pseudo (noncrystallographic) two-fold rotation axis to its partner within each pairing (Fig. 3a; pairings of molecules A/B and molecules C/D). These dimers are oriented with their planes approximately parallel with the crystallographic a axis (Fig. 3b).

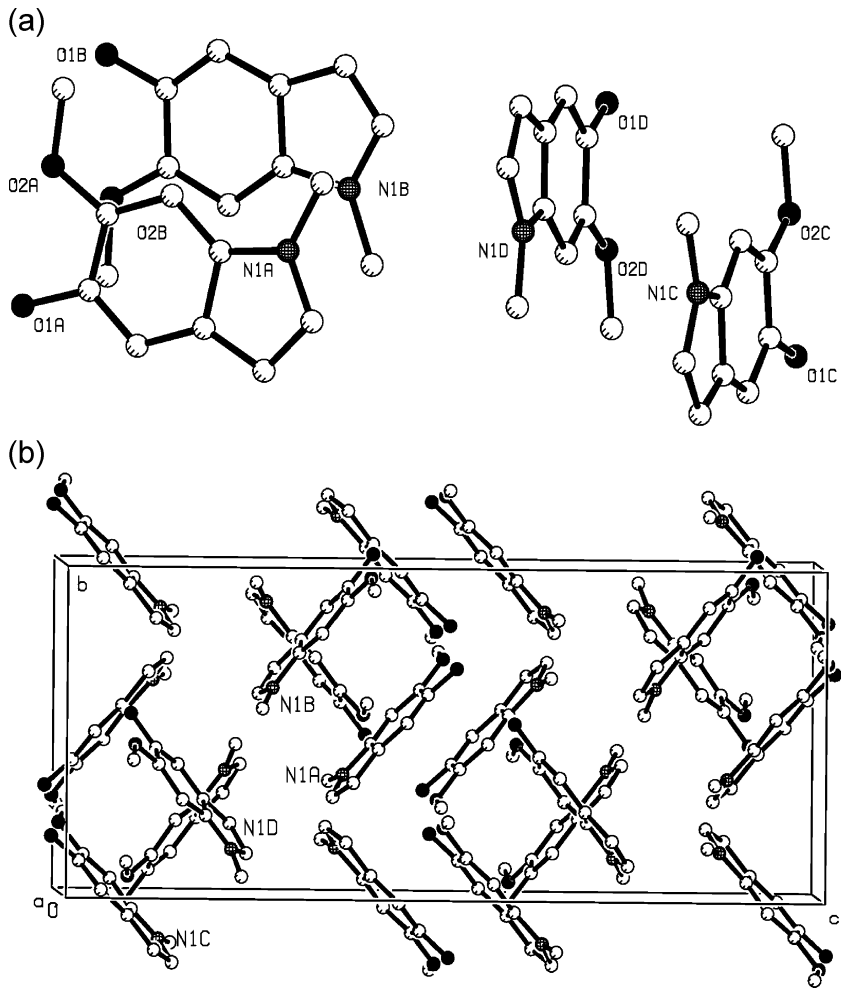

Figure 3. (a) The asymmetric unit of the crystal structure comprising four *N*-methyl-5-hydroxy-6-methoxyindole (MHMI) molecules organized into pairs (H atoms omitted for clarity). (b) PLATON diagram showing packing of the MHMI molecules parallel with (a).

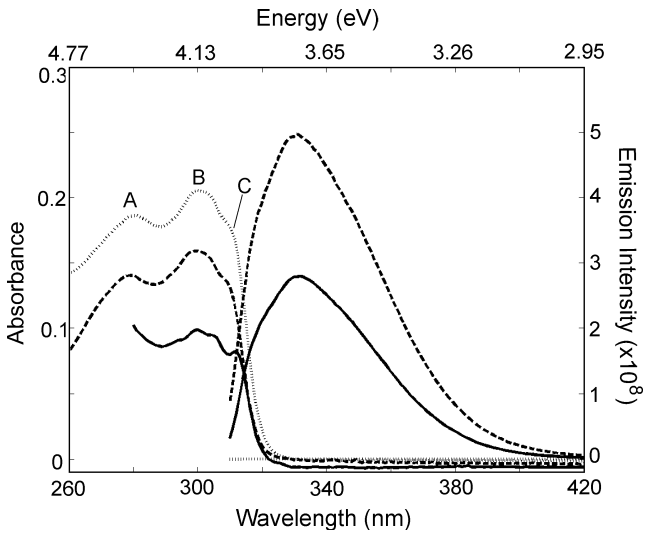

Figure 4. Absorbance and emission spectra for *N*-methyl-5-hydroxy-6-methoxyindole dissolved in benzene (solid line), acetonitrile (dashed line) and chloroform (dotted line). A = 279 nm (4.44 eV), B = 299 nm (4.15 eV), C = 311 nm (3.99 eV).

Optical absorbance and emission spectra for MHMI are shown in Fig. 4. The absorbance spectra are interesting in that they show two distinct peaks and a secondary shoulder. These features correspond to the energies 4.44 eV (279 nm), 4.15 eV (299 nm) and 3.99 eV (311 nm). The presence of two or more distinguishable peaks makes it similar to other indolic compounds, including DHI, *N*-acetyl-tryptophanamide (NATA) and indole-3-acetic acid (23–25). These peaks result from two distinct π-π^* transitions with overlapping vibronic bands (24). Although the absorbance spectrum of NATA has been shown to be slightly solvent dependent, no such dependence was observed in MHMI, suggesting that the electronic structure is not substantially affected by solvent interactions. In particular, they are virtually identical in acetonitrile and chloroform. In benzene, which is nonpolar, there is more apparent fine structure and a slight redshifting, particularly of the shoulder which now appears as a separate peak. It is also partially obscured by the strong absorbance of benzene as far as 280 nm.

The emission peaks are also similar in form, and the emission intensities (relative to the absorbance) are comparable in benzene and acetonitrile with quantum yields of 29% and 33%, respectively. This is also comparable to that of the

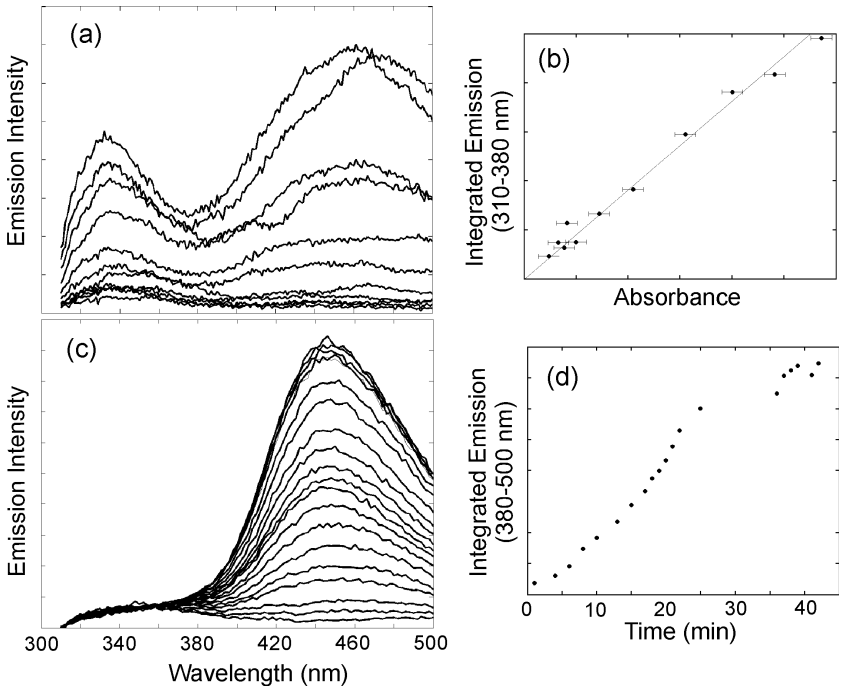

Figure 5. (a) Emission spectra of several *N*-methyl-5-hydroxy-6-methoxyindole concentrations in chloroform. (b) Plotting integrated emission against absorbance at 300 nm shows that the intensity of the peak centered at 335 nm scales with concentration. (c) Repeated emission spectra show that the intensity of the peak centered at 445 nm increases with UV exposure. (d) Integrated emission intensity increases approximately uniformly with each exposure. The emission intensity does not increase during intermediate time intervals without UV exposure.

DHICA monomer in DMSO (11). When dissolved in chloroform, however, the quantum yield is reduced to less than 1%. Closer inspection of the emission profiles in chloroform reveals two broad peaks, in contrast to the single peak observed in benzene and acetonitrile (Fig. 5a). Furthermore, the relative intensities of the peaks are not constant with either time or concentration. The short-wavelength peak intensity is linearly dependent on concentration (Fig. 5b), but the long wavelength peak is not.

In order to explore this further, we acquired a series of emission spectra on one sample, exciting at 300 nm. Increased exposure time to UV light had no effect on the short-wavelength peak, but caused a dramatic increase in intensity of the longer wavelength peak (Fig. 5c). It also turned the solution deep red and this was confirmed by the appearance of a broad peak centered at 530 nm in the absorbance spectrum. Time delays between UV exposures caused no increase in peak intensity, demonstrating that the transformation is photoactivated (Fig 5d). After a sufficient period of exposure, the peak intensity reached an asymptotic limit, suggesting that the chemical interactions had reached an equilibrium point. To test whether this increase in emission was a consequence of phenol oxidation, the experiment was repeated under a nitrogen atmosphere. Identical results were obtained, demonstrating that this emission is not caused by phenol oxidation.

DISCUSSION

We believe that the MHMI monomer created in our laboratory and studied here is an ideal compound for studying the impact of oligomeric size on the functional characteristics (*e.g.* spectroscopic properties) of indolic compounds. This compound is stable in solution, and highly soluble in a variety of solvents including DMSO and methanol in addition to those used here. It also crystallizes easily and forms only one form of dimer (through the 4-4′ positions), allowing clearer correlation of structure with spectroscopy. The methyl group attached to the nitrogen in the pyrrole ring forms a stable bond, inhibiting binding at the 2 position. Similarly, the methoxy group sterically hinders binding at the 7 position. Although recent work has demonstrated the existence of an indolic tetramer involving bonding in the 3 position (10), this position is still widely regarded not to contribute significantly to indolic polymerization and melanin formation *in vivo*. Absorbance spectra of the dimer show only one single discernible band, demonstrating that dimerization results in more closely spaced vibrational bands (Fig. 6). Proton NMR and crystallography results demonstrate that covalently coupled MHMI dimers synthesized in our laboratory were in fact connected in the 4 positions, and no interaction in the 3 position was observed (Fig. 7). More complete dimer data will be reported elsewhere. Stable MHMI polymers have also been formed, and these show a broad absorbance profile similar to that of eumelanin (Fig. 6). Due to the lack of diversity in the polymer constituents, however, the characteristic peak at 300 nm is still easily resolved. Preliminary studies of its ultrafast emission dynamics have already been reported (26).

Crystallographic data for the monomer confirm the molecular structure depicted in Fig. 1 and show that in the solid state, the two monomers facing each other are rotated 180° relative to each other around the long axis and slightly offset (Fig. 3b). The fact that the monomer forms this pairing arrangement, and

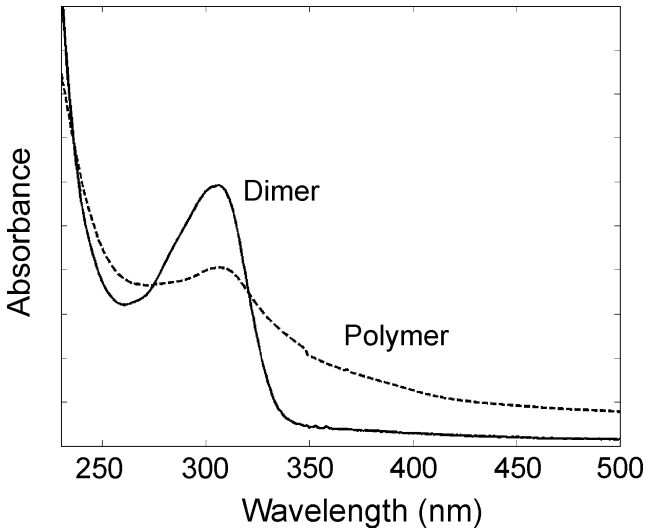

Figure 6. Absorbance spectra of the *N*-methyl-5-hydroxy-6-methoxy-indole dimer (solid) and polymer (dashed) in acetonitrile.

that the spacing is nearly identical to the spacing inferred from X-ray crystallographic studies of eumelanin, suggests that perhaps this arrangement is present in eumelanin as well. The fact that the monomer's radiative quantum yield in the liquid phase was substantial and comparable to that of DHICA indicates that pi-stacking was also negligible in solution in both benzene and acetonitrile. Thus, solvent aromaticity by itself does not affect the MHMI quantum yield. The comparable emission of MHMI to that of DHICA also demonstrates that addition of the methyl and methoxy groups in the 1 and 6 positions has little effect on quantum yields.

The reduced emission in chloroform is not caused by stacking, but the presence of two emission peaks suggested photoactivated creation of an excimer. Previous studies of NATA with chloroform demonstrated a strong chemical reaction between the excited state indole side chain and chloroform, resulting in a decrease in indole fluorescence and an increase in fluorescence at 480 nm, similar to that observed in Fig. 5c (27). The decrease in indole fluorescence seen here is very small but present, with an isosbestic point appearing at 360 nm. The reduced loss of emission intensity might be due to the presence of the hydroxy and methoxy groups. In Edwards *et al*. (27), appearance of the long-wavelength emission band was attributed to the binding of a chloroform derivative to the 5 position in indole.

However, the interaction observed here differs from that reported for NATA in two significant respects. First, as already noted, the decrease in indole fluorescence with irradiation is far less substantial than that for NATA. Second, ^{1}H NMR spectra of MHMI in d_4 methanol acquired before and after 2 h of UV irradiation (254 nm) in chloroform were nearly identical, except for the complete disappearance of the H-3 doublet and the collapse of the H-2 doublet into a singlet (data not shown). ^{13}C NMR spectra of the compound before

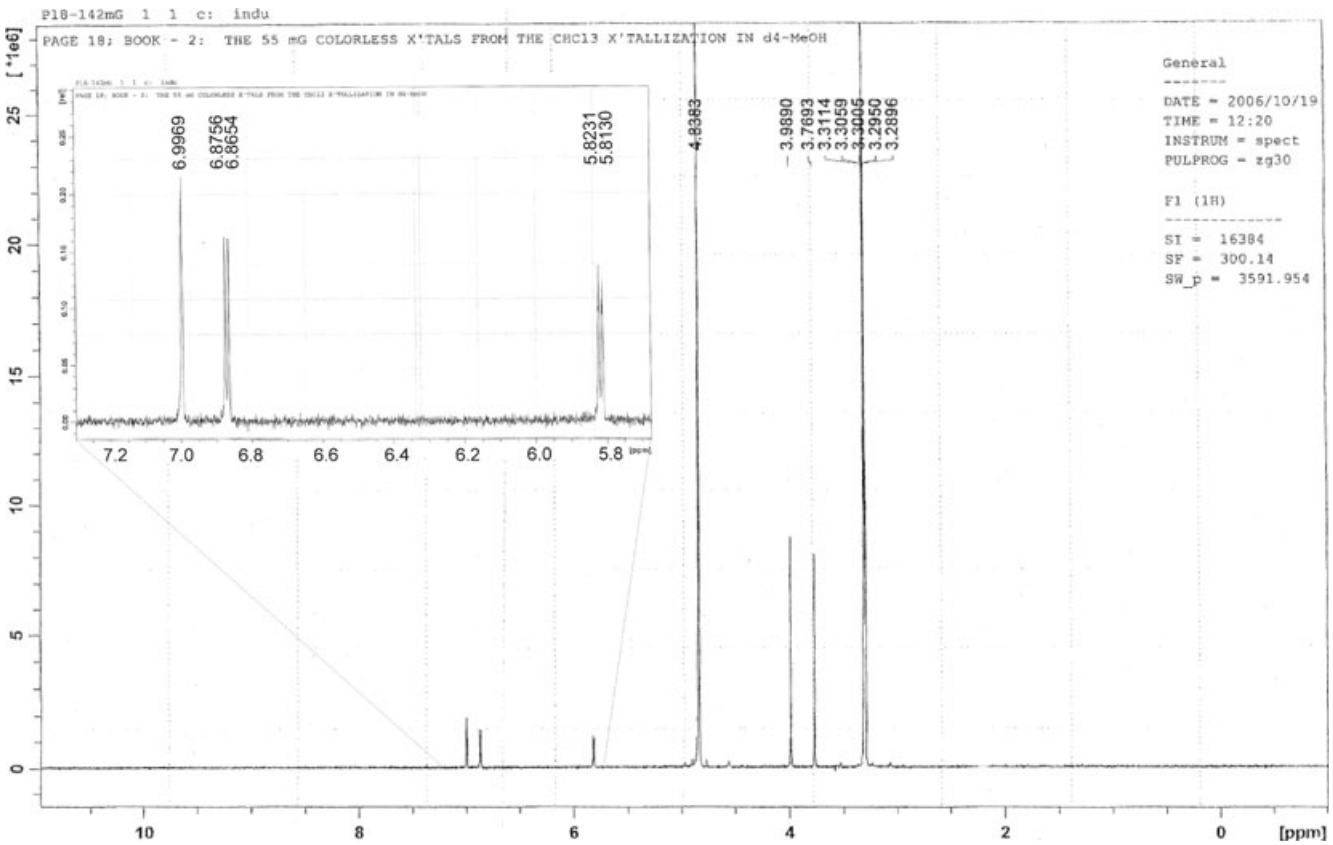

Figure 7. Proton NMR spectrum of the *N*-methyl-5-hydroxy-6-methoxyindole dimer in d_4 methanol. Signals at 5.8, 6.9 and 7.0 p.p.m. represent hydrogen atoms bound to the 3, 2 and 7 positions, respectively. Absence of the H-4 signal indicates that the dimer is bound only in the 4-4′ position.

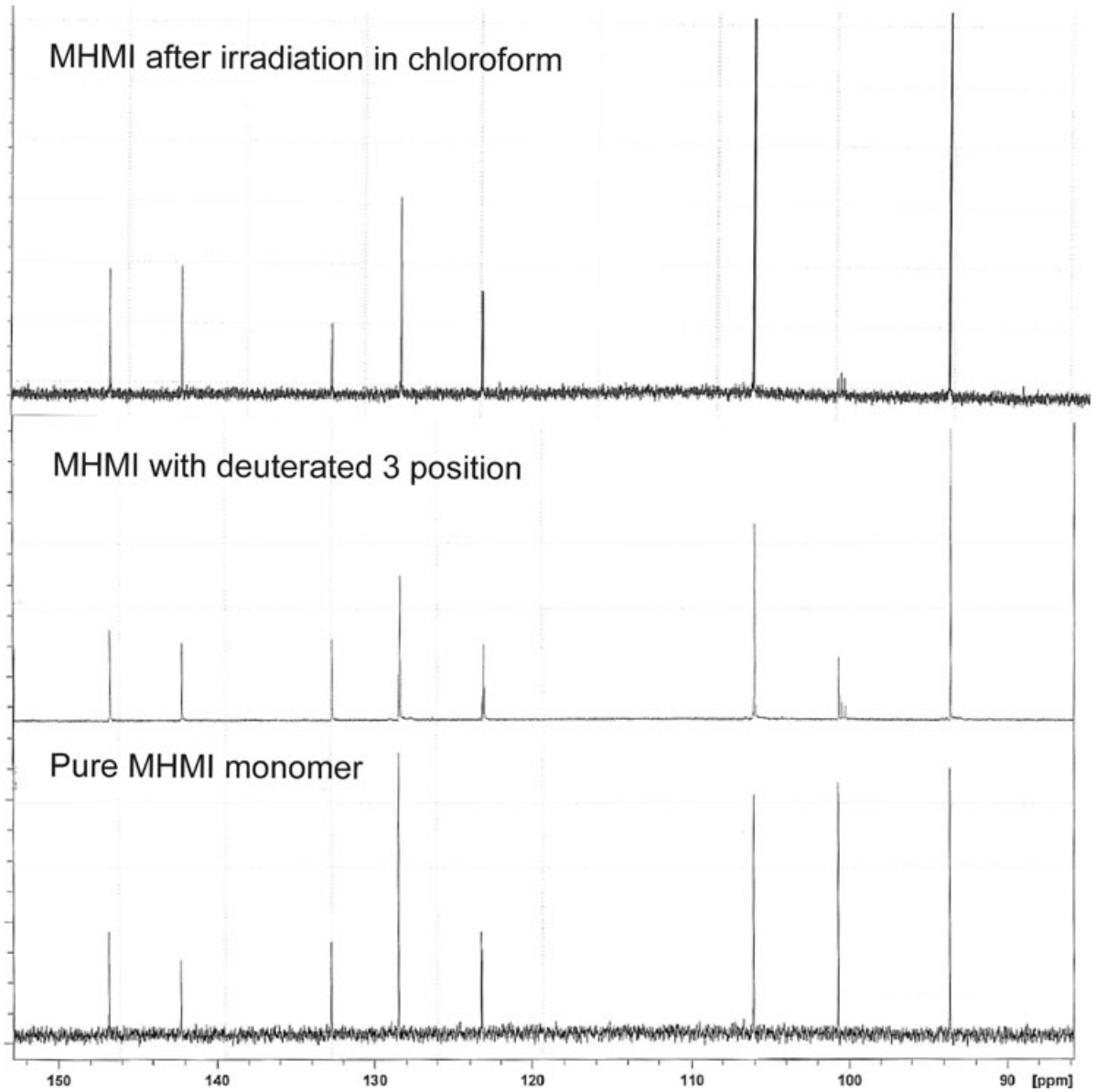

Figure 8. ^{13}C NMR spectra of the *N*-methyl-5-hydroxy-6-methoxyindole monomer in d_4 methanol in its pure form, after deuteration of the 3 position, and after irradiation in chloroform. Irradiation results in deuteration of the 3 position, causing a splitting of the peak at 100 p.p.m. into a triplet.

and after irradiation also show no change in signal positions except for the disappearance of the C-3 singlet at 100 p.p.m. and the appearance of a triplet at 100 p.p.m. because of deuterium exchange in d_4 methanol in the 3 position (Fig. 8). This deuterium exchange also explains the absence of the H-3 proton and the H-2 singlet in the irradiated species. If a chlorine derivative had bound to the monomer upon irradiation as observed for NATA, there would have either been a significant signal shift due to the electronegativity of chlorine or the appearance of an additional signal due to the presence of another carbon. The observation of neither suggests that there is no binding between the excited state indole and a chloroform derivative in this case, but rather that MHMI is more robust than other indolic compounds. In this case, it is possible that the negligible quantum yield in chloroform is the result of interactions such as hydrogen bonding between the indole and the solvent or excimer formation.

CONCLUSIONS

The MHMI monomer introduced here is well suited to the study of structure–function relationships in eumelanin, being stable in solid and liquid states, highly soluble in a variety of solvents and able to polymerize in a controlled, stepwise manner. Crystallographic examination reveals a unique structure in which four monomers are arranged in parallel pairs, spaced 3.5 Å apart, within each unit cell of the crystal. Optical spectra show it as having a multi-peaked absorbance profile and overlapping absorbance and emission spectra. More significantly, it exhibits strong fluorescence emission in solu-

tion with quantum yields of 29% and 33% in benzene and acetonitrile, respectively, similar to that of DHICA. However, like other indolic compounds, fluorescence is almost completely quenched in chloroform.

Acknowledgements—The authors thank Dr. Seth Olsen, Prof. Paul Burn and Prof. Halina Rubinsztein-Dunlop for helpful discussions, and Dr. Lynette Lambert and Mr. Ben Langley for help with the NMR and sample preparation. S.P.N.-R. was funded by a post-doctoral fellowship from Canada's Natural Sciences and Engineering Research Council and P.M. was funded by a Smart State Senior Fellowship from the Queensland State Government (Dept. of State Development).

REFERENCES

1. Sarna, T., B. Pilas, E. J. Land and T. G. Truscott (1986) Interaction of radicals from water radiolysis with melanin. *Biochim. Biophys. Acta* **883**, 162–167.
2. Nighswander-Rempel, S. P., J. Riesz, J. Gilmore and P. Meredith (2005) A quantum yield map for synthetic eumelanin. *J. Chem. Phys.* **123**, 194901.
3. Nighswander-Rempel, S. P., J. Riesz, J. Gilmore, J. P. Bothma and P. Meredith (2005) Quantitative fluorescence excitation spectra for synthetic eumelanin. *J. Phys. Chem. B* **109**, 20629–20635.
4. Stark, K. B., J. M. Gallas, G. W. Zajac, M. Eisner and J. T. Golab (2003) Spectroscopic study and simulation from recent structural models for eumelanin: II. Oligomers. *J. Phys. Chem. B* **107**, 11558–11562.
5. Stark, K. B., J. M. Gallas, G. W. Zajac, J. T. Golab, S. Gidanian, T. McIntire and P. J. Farmer (2005) Effect of stacking and redox state on optical absorption spectra of melanins—Comparison of theoretical and experimental results. *J. Phys. Chem. B* **109**, 1970–1977.
6. Meredith, P., B. J. Powell, J. Riesz, S. P. Nighswander-Rempel, M. R. Pederson and E. G. Moore (2006) Towards structure-property-function relationships for eumelanin. *Soft Matter* **2**, 37–44.
7. Del Vecchio, R. and N. V. Blough (2004) On the origin of the optical properties of humic substances. *Environ. Sci. Technol.* **38**, 3885–3891.
8. Kaxiras, E., A. Tsolakidis, G. Zonios and S. Meng (2006) Structural model of eumelanin. *Phys. Rev. Lett.* **97**, 218102.
9. Meredith, P. and T. Sarna (2006) The physical and chemical properties of eumelanin. *Pigment Cell Res.* **19**, 572–594.
10. Panzella, L., A. Pezzella, A. Napolitano and M. d'Ischia (2007) The first 5,6-dihydroxyindole tetramer by oxidation of 5,5′,6,6′-tetrahydroxy-2,4′-biindolyl and an unexpected issue of positional reactivity en route to eumelanin-related polymers. *Org. Lett.* **9**, 1411–1414.
11. Olsen, S., J. Riesz, I. Mahadevan, A. Coutts, J. P. Bothma, B. J. Powell, R. H. McKenzie, S. C. Smith and P. Meredith (2007) Convergent proton-transfer photocycles violate mirror-image symmetry in a key melanin monomer. *J. Am. Chem. Soc.* **129**, 6672–6673.
12. Tran, M. L., B. J. Powell and P. Meredith (2006) Chemical and structural disorder in eumelanins: A possible explanation for broadband absorbance. *Biophys. J.* **90**, 743–752.
13. Nofsinger, J. B. and J. D. Simon (2001) Radiative relaxation of sepia eumelanin is affected by aggregation. *Photochem. Photobiol.* **74**, 31–37.
14. Pezzella, A., A. Napolitano, M. d'Ischia and G. Prota (1996) Oxidative polymerisation of 5,6-dihydroxyindole-2-carboxylic acid to melanin: A new insight. *Tetrahedron* **52**, 7913–7920.
15. Pezzella, A., D. Vogna and G. Prota (2003) Synthesis of optically active tetrameric melanin intermediates by oxidation of the melanogenic precursor 5,6-dihydroxyindole-2-carboxylic acid under biomimetic conditions. *Tetrahedron Asymmetry* **14**, 1133–1140.
16. Farrugia, L. J. (1999) WinGX suite for small-molecule single-crystal crystallography. *J. Appl. Crystallogr.* **32**, 837–838.
17. Sheldrick, G. M. (1997) *SHELX-97—Programs for Crystal Structure Refinement, 97-2*. University of Goettingen, Goettingen.
18. Farrugia, L. (1997) ORTEP-3 for Windows. *J. Appl. Crystallogr.* **30**, 565.
19. Spek, A. L. (1990) Platon—A multipurpose crystallographic tool. *Acta Crystallogr. A* **46**, C34.
20. Nighswander-Rempel, S. P. (2006) Quantum yield calculations for strongly absorbing chromophores. *J. Fluoresc.* **16**, 483–485.
21. Demas, J. N. and G. A. Crosby (1971) Measurement of photoluminescence quantum yields—Review. *J. Phys. Chem.* **75**, 991–1024.
22. Cheng, J., S. C. Moss and M. Eisner (1994) X-ray characterization of melanins—II. *Pigment Cell Res.* **7**, 263–273.
23. Caric, D., V. Tomisic, M. Kveder, N. Galic, G. Pifat, V. Magnus and M. Soskic (2004) Absorption and fluorescence spectra of ring-substituted indole-3-acetic acids. *Biophys. Chem.* **111**, 247–257.
24. Lin, S. W. and T. P. Sakmar (1996) Specific tryptophan UV-absorbance changes are probes of the transition of rhodopsin to its active state. *Biochemistry* **35**, 11149–11159.
25. Zhang, X. Y., C. Erb, J. Flammer and W. M. Nau (2000) Absolute rate constants for the quenching of reactive excited states by melanin and related 5,6-dihydroxyindole metabolites: Implications for their antioxidant activity. *Photochem. Photobiol.* **71**, 524–533.
26. Nighswander-Rempel, S. P., I. B. Mahadevan, H. Rubinsztein-Dunlop and P. Meredith (2007) Time-resolved and steady state fluorescence spectroscopy of eumelanin and indolic polymers. *Photochem. Photobiol.* **83**, 1449–1454.
27. Edwards, R. A., G. Jickling and R. J. Turner (2002) The light-induced reactions of tryptophan with halocompounds. *Photochem. Photobiol.* **75**, 362–368.